Electronic Equalization of Fiber Optic Links

Andrew C. Singer, Naresh R. Shanbhag, and Hyeon-Min Bae
University of Illinois at Urbana Champaign, and Finisar Corporation, Inc.
Email: {acsinger,shanbhag}uiuc.edu, hyeonmin.bae@finisar.com

Abstract— **The days when optical fiber was viewed as having unlimited capacity have come to an end due to the steady growth in demand for bandwidth. Dispersion, noise and nonlinearities pose substantial channel impairments that need to be overcome. As a result, over the last decade, signal processing has emerged as a key technology to the advancement of low-cost high data rate optical communication systems. The unrelenting progress of semiconductor technology exemplified by Moore's Law provides an efficient platform for implementing signal processing techniques in the electrical domain leading to what is known as electronic dispersion compensation (EDC). In this paper, we provide an overview of some of the driving factors that limit the performance of optical links and provide a design example of an MLSE-based receiver for 10 Gb/sec long haul links.**

I. Introduction

The optical fiber has traditionally been thought to have near unlimited bandwidth. As a result, it has been the transmission media of choice in backbone networks and is rapidly making in-roads into customer premises, enterprise networks, as well as back-plane and storage area networks. As shown in Fig. 1, the key components of an optical fiber communication link are common to those of many digital communication links. Within the transmitter, an information sequence is used to modulate a laser source. For long-haul links (typically greater than 200 km), the optical signal will propagate along multiple spans of fiber with repeated optical amplification to overcome attenuation. In many regional or metro links (40 km to 200 km), the optical signal may propagate along a single span of fiber without additional amplification. In very short reach applications, the optical signal may only propagate a few tens to a few hunded meters through inexpensive, yet pervasive multi-mode (even plastic) fiber.

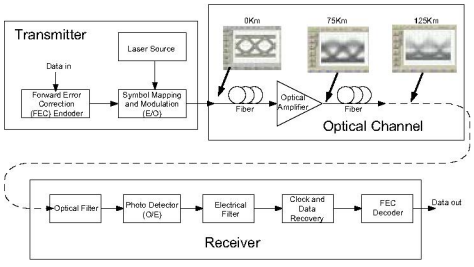

Fig. 1. Block diagram of an optical fiber link. The link can be broken into three key components: the transmitter, the optical channel, and the receiver.

While the data rates for optical links exceed those of all other digital communications media, in some respects, they remain among the least sophisticated, whereby nearly all deployed systems use simple on-off keying (OOK) and baseband comparators for symbol-by-symbol data recovery. This trend is likely to reverse itself, as a dramatic change in the nature of optical communications occurred earlier this decade when carriers began to migrate from 2.5 Gb/s to 10 Gb/s transmission rates. As a result of this transition, the performance of fiber optic links in long-haul, metro and enterprise networks became limited by dispersion, or intersymbol interference (ISI), rather than by noise. Figure 1 shows *eye diagrams* illustrating the transmitted and received symbol patterns as they would appear on an oscilloscope at various stages through the optical fiber.

This is largely because group-velocity dispersion (GVD), or so-called chromatic dispersion (CD), in optical fibers increases with the square of the data rate, and becomes a serious impairment at 10 Gb/s[1]. Polarization-mode dispersion (PMD), which arises from manufacturing defects, vibration, or mechanical stresses in the fiber, leading to additional pulse spreading at the receiver, also becomes serious in long-haul transmission at 10 Gb/s and at even shorter reaches for higher data rates. The time-varying nature of PMD gives rise to the additional need for adaptive compensation at the receiver. Modal dispersion, arising from geometrical properties of multi-mode fiber, are also considerably more severe at 10 Gb/s.

Electronic dispersion compensation (EDC) techniques have emerged as a technology of great promise for OC-192 (10 Gb/s) data rates and above. The remainder of this paper is structured as follows. In section II, a brief overview of system models is given. Specific attention is paid to channel models for single mode fiber and models for optical and electrical noise. Section III provides a case study of an MLSE-based adaptive receiver and some concluding remarks.

II. System Models

A. The Transmitter

The transmitter uses a binary data sequence to modulate the intensity (and possibly the carrier phase) of a laser source. The simple transmitter model in Fig. 2 describes the modulation process for a variety of applications. For example, the data source may be used to directly modulate the intensity of the laser driver, providing a simple on-off keyed (OOK) or non-return to zero (NRZ) modulation. While OOK is a form of linear pulse-amplitide modulation, NRZ is actually a nonlinear modulation in which the laser amplitude does not

[1]Long haul links at 2.5 Gb/s also need to have built-in dispersion compensation for GVD.

978-1-4244-1682-0/08/$25.00 ©2008 IEEE

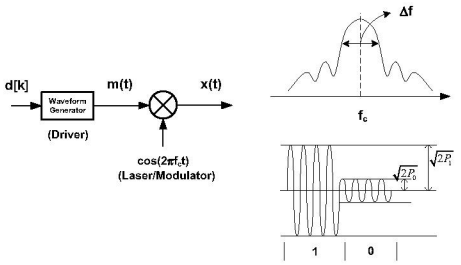

Fig. 2. A simple transmitter block diagram is shown in which an information sequence is used to modulate the intensity of a laser source. Also shown is the finite bandwidth of the laser about the carrier f_c and the finite extinction ratio of the modulated laser source.

return to zero, but rather remains on when successive *ones* are transmitted. As it is difficult to completely attenuate the optical signal at such high data rates, one measure of the quality of the laser is the *extinction ratio* (see Fig. 2), which is a measure in dB of the ratio of the optical power in a transmitted *one* to that in a transmitted *zero*, i.e., $E_r = 10\log_{10}\frac{P_1}{P_0}$. Direct modulation, for example, may achieve an extinction ratio as low as 8 dB, while external modulators achieve closer to 15 dB of extinction ratio. Note that a higher optical signal-to-noise ratio (OSNR) may not provide a lower BER, if the extinction ratio is poor.

B. The Fiber

After the data has been transmitted from the source and coupled into the optical fiber, it will propagate as an electromagnetic wave according to the nonlinear Schrödinger equation (NLSE) - the nonlinear wave equation governing the propagation of light in fiber [1] - and undergo a number of channel impairments. The propagating wave is supported by two orthogonal axes of polarization, or *polarization states* within the fiber. The differential group delay experienced by these two modes gives rise to polarization mode dispersion (PMD) causing pulse spreading at the output of the photodetector in the receiver. In multi-mode fiber (MMF) the transmitted signal will excite a number of propagating modes, which will propagate at mode-dependent velocities. This results in modal dispersion at the receiver, where a single transmitted pulse may spread into a number of adjacent symbol periods, depending on the data rate, the distance traveled, and the fiber properties. Single-mode fiber (SMF) permits only a single optical mode to propagate thereby enabling greater propagation distances before pulse spreading occurs. Long reach applications may include multiple spans of optical fiber that are periodically amplified using optical amplifiers. The noise induced by the optical amplifiers eventually becomes sufficiently large that the data integrity is in jeopardy, after the signal passes through a sufficient number of amplified fiber sections. At that point, optical-electrical-optical (OEO) regeneration is required whereby the signals are detected, converted to electrical format, error-corrected, and retransmitted through subsequent sections of optical fiber.

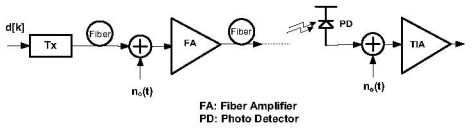

Fig. 3. Block diagram link model shows two primary sources of noise. The primary source of noise in an amplified link is amplified spontaneous emission (ASE) noise, indicated as *optical noise* $n_o(t)$, at the input the optical amplifier. In unamplified links, the dominant source of noise is the electrical receiver noise $n_e(t)$, which encompasses all sources of noise in the receiver, including that of the detector, the TIA and subsequent electronics.

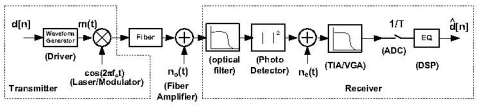

Fig. 4. An end-to-end system model for a fiber link is shown.

C. Noise Models

In amplified links, the dominant source of noise as observed at the receiver is amplified spontaneous emission noise, or ASE noise (see Fig. 3). At modest transmission powers, ASE noise can be modeled as additive, circularly symmetric, white complex Gaussian over the spectral bandwidth of the transmitted optical signal. The OSNR is computed as the ratio of the signal power in the transmitted optical signal to the ASE noise power in a reference bandwidth at a reference frequency adjacent to the transmitted signal. The typical noise reference bandwidth used is 0.1 nm, which is approximately 12.5 GHz for 1550 nm transmission.[2]

For directly detected optical signals, noise that was additive and Gaussian in the optical domain, becomes signal-dependent and non-Gaussian in the electrical domain. In particlar, denoting by $r(t)$ the output of the detector at time t and by $y(t)$ the noise-free output of the optical channel, it can be shown [2] that the conditional probability density function for $r(t)$ given the value of $y(t)$ is a signal-dependent non-central chi-square distribution with $2M$ degrees of freedom,

$$p_{r(t)}(r|y) = \frac{1}{N_0}\left(\frac{r}{y}\right)^{(M-1)/2} e^{\left\{-\frac{r+y}{N_0}\right\}} I_{M-1}\left(2\frac{\sqrt{ry}}{N_0}\right), \quad (1)$$

where N_0 is related to the average optical noise power over the bandwidth of the received optical signal, M is the ratio of the optical to the electrical bandwidth, and $I_k(.)$ is the kth modified Bessel function of the first kind.

D. End-to-End System Model

Figure 4 illustrates an end-to-end system model for an optical link, from transmitted information sequence to output detected symbol sequence. The process begins with the information sequence, which is mapped onto a modulating signal used to modulate the intensity of the laser source. The optical signal is then coupled into the optical fiber, which is modeled using either the linear CD model, MMF model,

[2]This is computed by noting that $f = c/\lambda$ and therefore $|\Delta f| = (c/\lambda^2)|\Delta\lambda| = 12.478GHz$, for $\lambda = 1550$ nm and $|\Delta\lambda| = 0.1nm$.

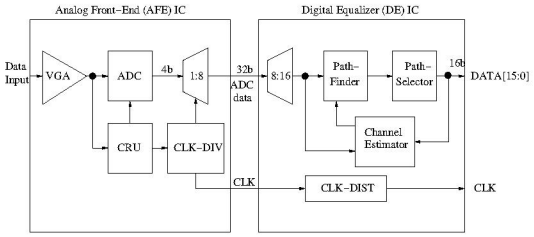

Fig. 5. Block diagram of MLSE-based receiver.

PMD model, or the NLSE model. The effect of any optical amplification is to introduce optical (ASE) noise, $n_o(t)$, into each of the polarization states of the optical signal. The optical signal is optically filtered and converted to an electrical signal (square-law detection), at which point electrical noise $n_e(t)$ is introduced from the detector-TIA-VGA chain, which also acts as a bandlimiting filter. The electrical signal is then sampled using a comparator or a multi-bit ADC from which the information sequence can then be estimated.

III. Case Study of an OC-192 EDC-based Receiver

Designing EDC-based receivers at OC-192 rates, i.e., 9.953 Gb/s to 12.5 Gb/s, poses numerous signal processing and mixed-signal circuit design challenges. In this section, we illustrate some of the issues that arise in implementing EDC using mixed-signal ICs by describing the design of a maximum likelihood sequence estimation (MLSE) receiver [3] with adaptive non-linear channel estimation. Key issues include: the design of a baud-sampled ADC, clock recovery in the presence of dispersion, non-linear channel estimation in the absence of a training sequence, and the design of a high-speed Viterbi equalizer. This is the first reported design of a complete MLSE receiver design meeting the specifications of OC-192/STM-64 long-haul(LH), ultra long-haul (ULH), and metro fiber links at rates up to 12.5 Gb/s.

A. MLSE Receiver Architecture

The MLSE receiver was designed as a two-chip solution in two different process technologies. The analog signal conditioning, sampling and clock recovery functions were implemented in an analog front-end (AFE) IC in a $0.18\,\mu$m, 3.3 V, 75 GHz, SiGe BiCMOS process. The digital MLSE equalizer and the non-linear channel estimator were implemented in a digital equalizer (DE) IC in a $0.13\,\mu$m, 1.2 V CMOS process.

The architecture of the MLSE receiver is shown in Fig. 5. The received signal is at a line rate of between 9.953 Gb/s for uncoded links and up to 12.5 Gb/s for FEC-based links. The received signal is amplified by a VGA then sampled by a 4-bit flash ADC. A dispersion-tolerant CRU recovers a line rate clock for the ADC. The 4-bit line rate ADC samples are demuxed by a factor of 1:8 to generate a 32-bit interface to the DE IC, which implements a 4-state MLSE algorithm, i.e. it assumes a channel memory of 3 symbol periods. The digital equalizer includes a blind, adaptive channel estimator using a volterra series expansion model for pattern-dependent impulse response and a data detection unit on-chip that requires no training.

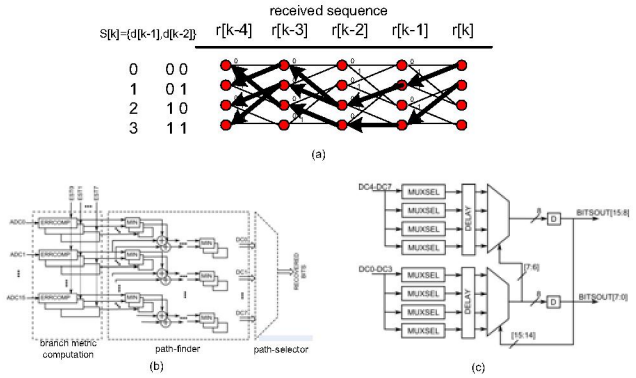

Fig. 6. High-speed MLSE: (a) time-reversed trellis, in which a cold-start at $r[k]$ leads to 4 possible reverse-survivor paths ending at states $s[k-D]$, (b) VLSI architecture, and (c) path-selector.

B. MLSE Equalizer Algorithm and VLSI Architecture

Designing an MLSE equalizer at OC-192 line rates (9.953 Gb/s-12.5 Gb/s) is extremely challenging because of the high data rates involved. Conventional high-speed Viterbi architectures often employ parallel processing or higher radix processing [4]. Parallel/block processing architectures tend to suffer from edge-effects while higher-radix architectures have been shown to achieve speed-ups of up to a factor of two, which is not sufficient for this application.

Instead, the architecture in [3, 5] (see Fig. 6) incorporates a number of techniques that enable the MLSE computations to complete within the bounds imposed by the high OC-192 line rates. First, the channel trellis is traversed in a time-reversed manner (see Fig. 6(a)). Doing so eliminates the trace-back step and the survivor memory associated with conventional approaches thereby providing a considerable power saving while enhancing throughput.

Second, the ACS bottleneck associated with conventional approaches is eliminated by restricting the survivor path memory to a reasonably small number of symbol periods. With a fixed survivor depth D, and time-reversed traversal of the trellis, it becomes possible to implement the ACS computations in a fully feed-forward architecture. This feed-forward ACS unit is referred to as the *path-finder* block in Fig. 6. A feed-forward architecture [6] can be easily pipelined in order to meet an arbitrary speed requirement.

Third, in order to avoid edge effects, past decisions are employed to select among the four possible survivor paths. Though this choice results in a recursive stage referred to as the *path-selector* (see Fig. 5) consisting of a series of multiplexers it is not difficult to meet the speed requirements. This is because the path-selector is a small and localized part of the architecture and hence easily amenable to circuit optimizations.

The three innovations described above provide a favorable trade-off between BER with ease of implementation. Though

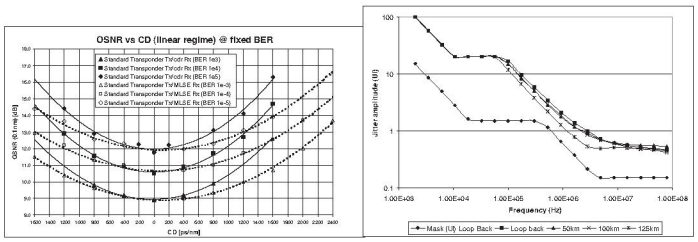

(a) (b)

Fig. 7. MLSE receiver test results: a) chromatic dispersion test, and b) SONET jitter tolerance.

these do not reduce frequency at which the architecture needs to be clocked, which remains at up to 12.5 GHz, they do result in an architecture that can be easily transformed into one that can operate at a lower clock-frequency as described next.

The fourth innovation is to make multiple (N_d) decisions along the chosen survivor path in each clock cycle resulting in a clock frequency that needs to be $1/N_d$ times the line rate. Fifth, the architecture is unrolled [6] in time by a factor of N_u resulting a further reduction of clock frequency by a factor of N_u. Thus, the final clock frequency is given by $f_{clk} = \frac{R}{N_u N_d}$ where R is the line rate. Algorithmically, unfolding [6] does not ease the throughput problem as it expands the number of computations in the critical path by the same factor as it lengthens the clock period. This fact does not present a problem in this case because the critical path is localized to the path-selector, which as mentioned earlier, is a simple cascade of multiplexers and hence can be custom designed to meet the speed requirements. A side benefit of making multiple decisions and employing unfolding is that the equalizer doubles up as a $1 : N_d N_u$ demultiplexer as well.

C. Measured Results

The MLSE receiver was tested with up to 200 km of SMF. The MLSE receiver achieves a BER of 10^{-4} at an OSNR of 14.2 dB with 2200 ps/nm of dispersion as shown in Fig. 7(a). A received power of -14 dBm is used throughout the testing. The MLSE receiver reduces the OSNR penalty of a standard CDR by more than 2 dB at 1600 ps/nm and BER of 10^{-4}. The penalty for a standard clock and data recovery (CDR) receiver, which simply recovers the clock using a PLL and makes symbol-by-symbol binary decisions through a comparitor, increases rapidly beyond 1600 ps/nm of CD. Figure 7(a) also shows that the MLSE receiver does not have a penalty in the back-to-back (i.e. 0 km) configuration.

In [7], another group reports results for an MLSE receiver for rates up to 10.7 Gb/s, however that MLSE recevier appears to have a 2dB OSNR penalty at back to back, i.e. in the absence of dispersion. As a result, the measured results in [3] are better than those in [7] by $2dB$ over the range of dispersion from back-to-back through 1600ps/nm, after which the results coincide.

The receiver has been shown to provide an error free (BER $< 10^{-15}$) post-FEC output, with a pre-FEC BER of 10^{-3} at 10.71 Gb/s with 2000 ps/nm of dispersion. It can compensate for 60 ps of instantaneous differential group delay (DGD) with a 2 dB OSNR penalty (BER=10^{-6}). The channel estimator in the MLSE engine adapts at a rate of 30 MHz and thus is easily able to track variations in DGD, which are typically less than 1 KHz.

The MLSE receiver satisfies the SONET jitter tolerance specifications with 2200 ps/nm of dispersion (see Fig. 7(b)). A HP OMNIBER OTN is used for this measurement. The measured output clock jitter is $< 0.5\,\mathrm{ps_{rms}}$. The output BER is kept at 10^{-3} and the CD is varied up to 2200 ps with a $2^{31}-1$ PRBS. The fixed BER is achieved by adjusting the OSNR while maintaining the received optical power at -14 dBm. The PLL output clock jitter is less than $0.64\,\mathrm{ps_{rms}}$ across test conditions. The PLL remains locked without cycle slips with up to 1300 consecutive identical digits (CID) at a BER of 10^{-2}, with a 125 km SMF-28 optical fiber link.

The MLSE receiver illustrates the benefits of jointly addressing signal processing algorithm design, VLSI architectures, mixed-signal integrated circuit implementation, as well as electromagnetic signal integrity issues in packaging and circuit board design.

IV. Concluding Remarks

The potential for electrical signal processing to enhance the performance of optical links has been discussed for decades, dating at least as far back as the work of Personick [8], who provided a system theoretic analysis of receiver design for optical systems. Some early work [9] discussed optimal detection of optical signals and even considered the potential future design of such receiver structures. With the tremendous advances in semiconductor technology and EDC-based products making their way into commercial systems, it appears that this time has come.

References

[1] G. P. Agrawal, *Fiber-Optic Communication Systems.* Wiley-Interscience, 2002.

[2] P. Humblet and M. Azizoglu, "On the bit error rate of lightwave systems with optical amplifiers," *Journal of Lightwave Technology*, vol. 9, pp. 1576–1582, November 1981.

[3] H. M. Bae, J. Ashbrook, J. Park, N. Shanbhag, A. C. Singer, and S. Chopra, "An MLSE receiver for electronic-dispersion compensation of OC-192 links," *Journal of Solid-State Circuits Conference, Journal of Solid State Circuits*, vol. 41, pp. 2541–2554, November 2006.

[4] P. J. Black and T. H. Meng, "A 140-Mb/s, 32-state, radix-4 Viterbi decoder," *IEEE Journal of Solid-State Circuits*, vol. 27, pp. 1877–1885, Dec. 1992.

[5] R. Hegde, A. Singer, and J. Janovetz, "Method and apparatus for delayed recursion decoder," *US Patent*, no. 7206363. filed June, 2003, issued April, 2007.

[6] K. K. Parhi, *VLSI Digital Signal Processing Systems: Design and Implementation.* Wiley, 1999.

[7] A. Farbert, S. Langenbach, N. Stojanovic, C. Dorschky, T. Kupfer, C. Schulien, J.-P. Elbers, H. Wernz, H. Griesser, and C. Glingener, "Performance of a 10.7 Gb/s receiver with digital equaliser using maximum likelihood sequence estimation," *ECOC'2004 Proceedings*, pp. PD–Th4.1.5, 2004.

[8] S. Personick, "Receiver design for digital fiber optic communication systems," *Bell Systems Technical Journal*, vol. 52, July,August 1973.

[9] G. Foschini, R. Gitlin, and J. Salz, "Optimum direct detection for digital fiber optic communication systems," *Bell Systems Technical Journal*, vol. 54, October 1975.